Characterization of egg white gel microstructure and its relationship with pepsin diffusivity

Geeshani Somaratne, Francoise Nau, Maria J. Ferrua, Jaspreet Singh, Aiqian Ye, Didier Dupont, R. Paul Singh, Juliane Floury

Food Hydrocolloids 98 (2020) 105258

Contents lists available at ScienceDirect

Food Hydrocolloids

journal homepage: www.elsevier.com/locate/foodhyd

Characterization of egg white gel microstructure and its relationship with pepsin diffusivity

Geeshani Somaratne[a,b], Francoise Nau[c], Maria J. Ferrua[a,d], Jaspreet Singh[a,b], Aiqian Ye[a], Didier Dupont[c], R. Paul Singh[a,e], Juliane Floury[c,*]

[a] Riddet Institute, Massey University, Palmerston North, New Zealand
[b] Massey Institute of Food Science and Technology, Massey University, Palmerston North, New Zealand
[c] STLO, INRA, AGROCAMPUS OUEST, 35042, Rennes, France
[d] Fonterra Research and Development Centre, Palmerston North, New Zealand
[e] University of California, Davis, CA, USA

ARTICLE INFO

Keywords:
Pepsin
Diffusion coefficient
Egg white gel
FRAP
Electrostatic interactions

ABSTRACT

Understanding the diffusion of digestive enzymes, particularly pepsin, in different food structures, is a key factor to better control protein digestion and absorption. This study aimed to investigate how protein-based food microstructure impacts pepsin diffusion. Two egg white gels (EWGs) of identical protein concentration (10%) but different structures were used as food models. The two different gel structures were prepared by heating liquid egg white at pH5 and pH9, respectively. Results showed that egg white proteins formed a compact and microstructurally homogeneous gel at pH9 (mean particle size of 0.32 ± 0.02 μm, with a mean interparticle distance of 0.76 ± 0.07 μm), which leads to a lower FITC-pepsin diffusion coefficient (D_{eff} = 44.2 ± 6.1 $\mu m^2 s^{-1}$), compared to the pH5-EWG (D_{eff} = 52.5 ± 5.3 $\mu m^2 s^{-1}$). The microstructure of the pH5-EWG was characterised by a spatially heterogeneous loose protein matrix made of larger aggregate particles (mean particle size of 0.76 ± 0.07 μm, with a mean interparticle distance of 1.79 ± 0.57 μm). In addition to the effects of the EWG microstructure, the environmental pH also affects the FITC-pepsin diffusion, likely because of the impact on electrostatic interactions between pepsin and the egg white proteins.

1. Introduction

Proteins, when present as a main constituent in a food matrix, are important for their nutritional properties and various functionalities such as gelling, emulsifying and foaming abilities (Foegeding & Davis, 2011). Digestion of food protein initiates in the stomach by the action of pepsin (Akimov & Bezuglov, 2012; Inglingstad et al., 2010). The mobility of pepsin into food matrices and their subsequent breakdown in the gastric environment are strongly correlated with the food matrix structure (Guo et al., 2015; Luo, Borst, Westphal, Boom, & Janssen, 2017; Nyemb, Guérin-Dubiard, et al., 2016; Thevenot, Cauty, Legland, Dupont, & Floury, 2017). Since food structure can have a critical role in determining the rate of peptide release in the stomach and absorption of amino acids/peptides in the small intestine, it is of ultimate importance to nutrition and health (Lorieau et al., 2018; Luo et al., 2017; Nyemb, Causeur, et al., 2016; Nyemb, Guérin-Dubiard, et al., 2016).

Egg white proteins mainly including ovalbumin, ovotransferrin, ovomucoid and lysozyme, are widely available and show a well-balanced profile of amino acids with high bioavailability (Abeyrathne, Lee, & Ahn, 2013; Matsuoka, Takahashi, Kimura, Masuda, & Kunou, 2017). Besides their nutritional characteristics, the denaturation and aggregation behaviour of these proteins is of particular relevance toward manufacture of hydro- or emulsion gel structures which can act as nutrients or drug delivery systems (Drakos & Kiosseoglou, 2006; Opazo-Navarrete, Altenburg, Boom, & Janssen, 2018; Tomczyńska-Mleko et al., 2016). Without altering the protein composition of egg white, changes in pH and ionic strength, followed by heat treatment can produce gels with varying macro- and micro-structural designs (Nyemb, et al., 2016a,b). Thus, egg white gels (EWGs) provide interesting protein-based model food for investigating the food matrix effect on the diffusion kinetics of pepsin into food matrices.

A number of studies have provided evidence that the structure of egg white protein gelled with different pH conditions play a predominant role in their rate of *in-vitro* and *in-vivo* protein digestion as well as in the nature of peptides released (Nyemb, Causeur, et al., 2016; Nyemb, Guérin-Dubiard, et al., 2016; Nyemb, Rutherfurd, Guérin,

* Corresponding author. Agrocampus Ouest, INRA, UMR, 1253 Science et Technologie du Lait et de l'Œuf, 65 rue de St Brieuc, 35012, Rennes Cedex, France.
E-mail address: juliane.floury@agrocampus-ouest.fr (J. Floury).

https://doi.org/10.1016/j.foodhyd.2019.105258
Received 1 February 2019; Received in revised form 10 July 2019; Accepted 30 July 2019
Available online 05 August 2019

Dupont, & Nau, 2015). Furthermore, these findings reported the microstructure of EWGs using transmission electron microscopy (TEM) and scanning electron microscopy (SEM) and demonstrated its impact on the digestion behaviour of these protein gels (Nyemb, Guérin-Dubiard, et al., 2016). However, there are no systematic studies in the literature aimed at quantitative description of the microstructure of the EWGs and their impact on the gastro-intestinal digestion. This is partly due to a lack of appropriate techniques for undisturbed visualization and quantification of dense microstructures of EWGs at an appropriate high resolution. The other unexplored aspect of the previous findings is the extent and rate to which digestive enzymes, particularly gastric pepsin can penetrate into the gel microstructure and contribute to hydrolyse the protein in EWGs.

Recent advances in confocal laser scanning microscopy (CLSM) and in fluorescent tracers make it possible to quantitatively characterize the microstructure and diffusion rate of digestive enzyme within food matrix. The Airyscan technology was recently introduced by ZEISS using a new detector concept for CLSM. It mainly replaces the physical pinhole aperture with a 32-channel area detector to acquire a pinhole-plane image at each and every scan position (Huff, 2015). Thereby, this approach allows to enhance both the spatial resolution and signal-to-noise-ratio (SNR) information of the micrographs, without increasing the excitation power and image acquisition time by averaging of multiple images, as it is often the case in conventional confocal microscopy (Huff, 2015; Korobchevskaya, Lagerholm, Colin-York, & Fritzsche, 2017). To our knowledge, this super resolution imaging technique has never been applied for EWG microstructure observation. Yet it could allow visualization and quantification of the morphological features of the microstructures of EWGs by simply using fluorescent dyes for labelling the egg white proteins. This technique could therefore represent an interesting alternative to other imaging techniques requiring laborious preparation of samples such as electron microscopy.

Fluorescence recovery after photobleaching (FRAP) is a widely established CLSM based method for the estimation of effective diffusion coefficients of fluorescently labelled molecules. It has recently been used to study the mobility of the digestive enzymes within the food matrix (Guo, Bellissimo, & Rousseau, 2017; Thevenot et al., 2017). Techniques related to confocal microscopy including FRAP and fluorescence correlation spectroscopy (FCS) have been used to characterize the diffusion of pepsin in different dairy-based gel microstructures (Luo et al., 2017; Thevenot et al., 2017). Luo et al. (2017) have shown that the architecture of the dairy-based gel matrix could affect the overall proteolysis reaction rate and the gels breakdown properties. However, the diffusion of pepsin into protein-based gel matrix depends on the type of protein and thus, it is required to investigate the pepsin diffusivity within the individual sources of protein.

With all the above background information, the objectives of the present study were to gain further understanding on the microstructural characteristics of egg white protein gels (pH5 and pH9 EWGs) using a high-resolution confocal microscopy, and to identify how the diffusion properties of fluorescently labeled FITC-pepsin and FITC-dextran (40 kDa) is affected by the EWG matrices using the FRAP technique. In particular, the microstructural parameters of model foods were qualitatively related to the diffusivity of FITC-pepsin. The diffusivity of FITC-dextran (40 kDa) was used to identify any electrostatic interactions (if presence) between the egg white proteins and FITC-pepsin.

2. Materials and methods

2.1. Materials

Fresh eggs were purchased from a local supermarket (Rennes, France). The total protein (N × 6.25) in the egg white was determined using the Kjeldahl method. Fast Green, pepsin from porcine gastric mucosa, Fluorescein isothiocyanate (FITC), and FITC–dextran of the average molecular weight of 40 kDa were purchased from Sigma-Aldrich (St. Louis, MO, USA). Pepsin was labelled with FITC as described in section 2.3. The FITC-pepsin was used to evaluate the diffusion rate of pepsin within the different EWG structures. The FITC–-dextran was dissolved in sterile water to a concentration of 50 mg/mL and used to investigate the diffusion rate of a chemically inert molecule within the EWG matrices. All the reagents used were analytical grade.

2.2. Preparation of EWGs

The eggs were manually broken and the egg whites were carefully separated from the yolks. The whole egg white solution (250 mL) was homogenized using an IKA T-18 Ultra Turrax Digital Homogenizer (10,000 rpm for 1 min). Two sub-samples of 30 mL egg white solution were taken and the pH of each sub-sample was adjusted to pH 5.0 or pH 9.0, respectively, using 2M HCl or 2M NaOH. Egg white solutions were then diluted with Milli-Q water to 10% protein concentration.

For gel microstructure study, about 600 μL of the pH5 or of the pH9 egg white solution were poured into 1 mL Eppendorf tubes. They were mixed with 6 μl aliquot of 1% (wt/v) of Fast Green. The mixture was vortexed, and then each solution (100 μL) was slowly injected into the chamber of an IBIDI μ-Slide I Luer system (IBIDI GmbH, Martinsried, Germany). The IBIDI system was then covered using aluminum foils to prevent photo-bleaching of fluorescent molecules.

For the FRAP analysis, about 150 μL of each egg white solution were poured into the individual wells of an open IBIDI μ-Slide (chambered coverslip) with 8 wells system (IBIDI GmbH, Martinsried, Germany), and covered with a coverslip.

In both cases, the IBIDI systems were horizontally heated at 80 °C for 5 min in a temperature-controlled water bath. After heating, the samples were cooled to room temperature and stored at 19 °C in an air-conditioned room until measurements.

2.3. Pepsin labeling

For the FRAP analysis, pepsin was labeled with FITC according to the manufacturer's instructions as described in a previous study (Thevenot et al., 2017). Briefly, pepsin was first dissolved at a concentration of 0.27 mM in a 10 mM phosphate buffer solution (pH 8.0). Pepsin was covalently labeled with FITC by mixing 1.8 mL of a FITC solution (38 mM FITC) with 100 mL of the protein solution for 90 min at room temperature and protected from light. The solution of FITC-pepsin was then dialyzed with cellulose membranes with a nominal cutoff of 6–8 kDa (Spectrum Laboratories, Canada) against 10 mM Tris/0.6 M NaCl buffer (pH 7.33) for 2 days to eliminate any remaining free FITC. A final purification step using dialysis was made by using deionized water. The pepsin inactivation by the labelling reaction was checked by measuring the FITC-pepsin activity using haemoglobin (Hb) as the substrate according to the method described in Minekus et al. (2014). The FITC-pepsin was dissolved in sterile water to a concentration of 50 mg/mL.

2.4. Confocal imaging

The EWGs labeled with Fast Green were imaged with the inverted LSM 880 confocal laser scanning microscope (Carl Zeiss AG, Oberkochen, Germany) using the Airyscan detection unit. To maximize the resolution enhancement, a Plan Apochromat 63x with high numerical aperture (NA = 1.40) oil objective was used. A He/Ne laser with a wavelength of 633 nm was used to excite the Fast Green dye, with appropriate emission in each system. Laser power, detector gain and pixel dwell times were adjusted for each dataset keeping them at their lowest values in order to avoid saturation and bleaching effects.

Airyscan images were acquired with 7% of the maximum with a main beam splitter MBS488/561/633, no additional emission filter, a gain setting of 700–780, a pixel dwell time of 1.54 μs and no averaging. The zoom was automatically set at 1.8 as requested by the system. For

further image analysis, at least ten micrographs of 1336x1336 pixels (1 μm = 18.17 pixels) were taken on different regions in a constant z-position (at a depth of 8 μm from the surface) of three independent samples of each of the two EWGs.

Zen Black 2.1 (Version 13.0.0.0) software was used to process the acquired datasets using the 2D mode at default settings of the Airyscan processing function. The software processes each of the 32 Airy detector channels separately by performing filtering, deconvolution and pixel reassignment in order to obtain images with enhanced spatial resolution and improved SNR. This processing includes a Wiener filter deconvolution with options of either 2D or a 3D reconstruction algorithm as described in Huff (2015).

2.5. Image analysis

The microstructure of the EWGs were characterized from the Airyscan confocal micrographs using FIJI software and according to the image analysis technique previously described by Silva, Legland, Cauty, Kolotuev, and Floury (2015a) with slight modifications. The egg white protein network was enhanced using a white top-hat filter by removing the artifacts, and smoothening was done to remove acquisition noise. The enhanced image was converted to a binary image using the Otsu thresholding algorithm with egg white protein phase contributing black pixels and aqueous phase contributing white pixels. The segmentation procedure was validated by visual comparison of the resulted binary image with its original image. Fig. 1 shows the schematic representation of the confocal micrographs segmentation procedure.

Quantification of microstructural parameters was performed using MorphoLibJ, Granulometry and Geodesics plugins as previously reported in Legland, Arganda-Carreras, and Andrey (2016); Legland, Devaux, Bouchet, Guillon, and Lahaye (2012); Silva et al. (2015a) and Thevenot et al. (2017). Five different microstructural parameters were determined. They are particle area fraction (ratio between the protein matrix area with respect to the total area of the image), boundary length per unit area (ratio between the length of the perimeter around all the protein particle aggregate edges or boundaries with respect to the total image area), size of particle aggregates, inter-particle aggregate distances and the tortuosity parameter, which is defined as the ratio of the actual flow path length through the pores to the shortest distance between the beginning and the end of the flow path (the Euclidean distance) (Silva et al., 2015a; Thevenot et al., 2017).

2.6. FRAP analysis

Effective diffusion coefficients (D_{eff}) of fluorescently-labelled pepsin, as well as labelled dextran within EWGs were determined using an adaptation of the FRAP protocol described by Floury, Madec, Waharte, Jeanson, and Lortal (2012) and Thevenot et al. (2017). EWGs were prepared in the individual wells of an open IBIDI μ-Slide system as described earlier (section 2.2) and then a 20 μL aliquot of 50 mg/mL FITC-pepsin and FITC-dextran (40 kDa) was added to the surface of the gel sample. To ensure fluorescent molecules to migrate from the surface of the gel toward the bottom of the sample, the samples were kept at room temperature (20 °C) for approximately 30 min before measuring. For each gel type, three different gels were prepared separately to ensure the reproducibility of the gel-processing stage.

The FRAP analysis was performed on the CLSM (Zeiss LSM880, Oberkochen, Germany). All diffusion measurements were performed at 20 °C in an air-conditioned room. The FITC-pepsin and the FITC–dextran were excited using argon laser system at a wavelength of 488 nm and detected on a 495–580 nm spectral bandwidth. The 488 nm argon laser was set to between 0.5 and 5% for imaging and 100% for bleaching step. The pinhole was set to 1 airy unit. Samples were observed at a constant depth of 15 μm from the sample surface using a 40 × objective lens (oil immersion) with a numerical aperture of 1.30. The bleached region was a circular region within each image with a

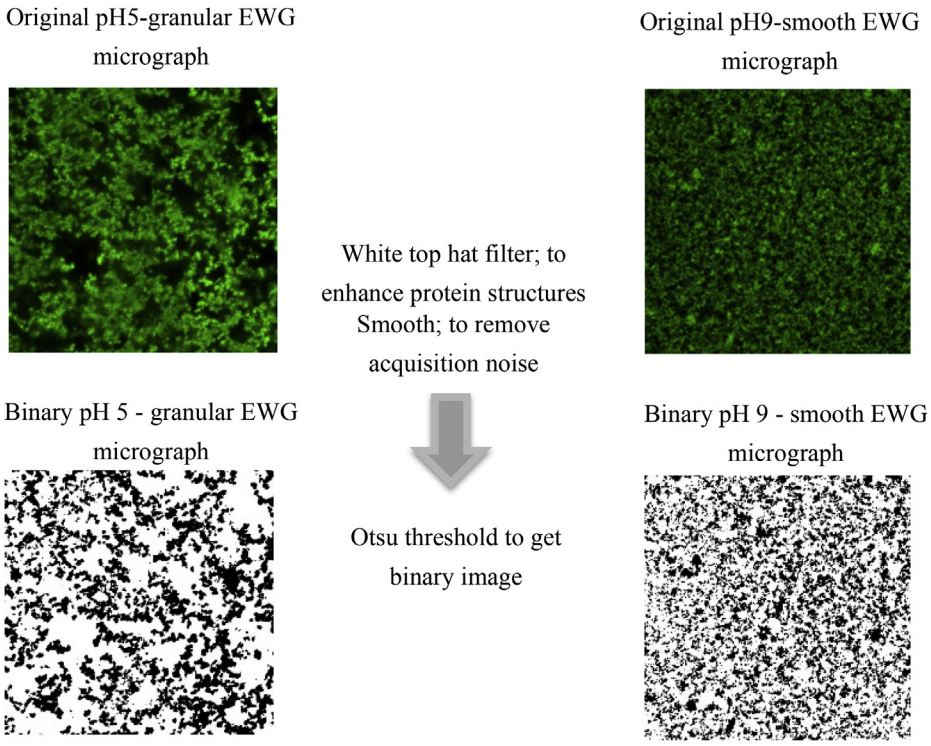

Fig. 1. Schematic representation of the confocal micrographs segmentation procedure.

radius of 5 μm. A rectangle region was selected as the background. The bleached region was scanned with 20 pre-bleach images, and then bleached with 150 iterations followed by fluorescence recovery. A total of 480 images were captured during post-bleaching at 0.1 ms intervals until full recovery was reached. Ten FRAP acquisitions were carried out on the different locations of each EWG.

Control FRAP experiments were achieved in the same conditions in water with the FITC-dextran (40 kDa) and FITC-pepsin with a concentration of 0.5 mg/mL, according to the method as described in Silva, Lortal, and Floury (2015b). Briefly, the fluorescent water (100 μL) was poured between a glass slide and a cover slip sealed with an adhesive frame (Geneframe, ABgene House, UK).

Data were analyzed by using the analytical method described in Thevenot et al. (2017) with the assumptions of pure isotropic diffusion in a homogeneous medium and a two-dimensional diffusion process using the classical diffusion equation given by the Fick's second law (supplementary material). Analyses of the recorded images were performed using FIJI software and the effective diffusion coefficients (D_{eff}) were obtained by data fitting via nonlinear least squares with RStudio software. The reduced diffusion coefficient was calculated as the ratio of effective diffusion coefficient for the FITC–pepsin or FITC–dextran in the gel matrix divided by the diffusion coefficient of the same probe in water.

2.7. Statistical analysis

The Student's test was applied in order to compare the microstructural parameters of the two EWGs. One-way analysis of variance (ANOVA) and Tukey's paired comparison test were applied to the diffusion coefficient data of the two different EWGs and water to determine which mean values were significantly different from one another at the 95% confidence level. The statistical analysis was performed using R software (R 3.1.2, Project for statistical computing).

3. Results and discussion

3.1. Observation of EWGs microstructure

The EWG microstructure can be defined as the arrangement of egg white protein aggregate particles. Fig. 2 shows the two different EWGs (pH5 and pH9) micrographs obtained from confocal imaging. Thanks to Fast Green labelling, proteins appear coloured in green on the confocal micrographs, while associated pores in aqueous phase appear in black.

As shown in micrographs, the microstructural organization strongly differs between pH5-EWG (Fig. 2a) and pH9-EWG (Fig. 2b). When the pH is adjusted to pH5 before heat gelation, egg white produced a more porous, loosely packed and heterogeneous protein network. Conversely, when the pH of egg white solution is adjusted to pH9, it produced a dense and more homogeneous protein network. This result was in precise agreement with earlier reported SEM and TEM observations for pH5 - granular and pH9 - smooth EWGs microstructure (Nyemb, Guérin-Dubiard, et al., 2016). These authors also observed large spherical aggregates in pH5-EWG, and both small spherical and linear aggregates in pH9-EWG.

Table 1
Quantitative parameters characterizing the microstructure of pH5 and pH9 EWGs obtained from image analysis on binary confocal micrographs. The results are expressed as the mean ± SD (n = 30); *indicates the means within a single row are significantly different ($p < 0.05$).

Parameter	pH5-EWG	pH9-EWG
Particle area fraction	0.31 ± 0.08	0.29 ± 0.02
Boundary length per unit area (μm/μm^2)	0.92 ± 0.20	1.93 ± 0.11*
Tortuosity	1.14 ± 0.14*	1.07 ± 0.01
Particle aggregate size (μm)	0.76 ± 0.07*	0.32 ± 0.02
Inter-particle aggregate distance (μm)	1.79 ± 0.57*	0.76 ± 0.07

3.2. Microstructural parameters of native EWGs

From the series of micrographs of each gel microstructure, particle area fraction, boundary length per unit area and tortuosity were calculated (Table 1). Particle area fractions were not statistically different ($p > 0.05$) between the pH5 and pH9 EWGs. This result is not surprising because the protein concentration was the same in both gels (10%). However, the boundary length per unit area was significantly ($p < 0.05$) larger for the pH9-EWG (1.93 ± 0.11 μm/μm^2) than for the pH5-EWG (0.92 ± 0.20 μm/μm^2), consistently with the significantly smaller particle size at pH9 when compared to pH5. Indeed, the mean particle size was 0.76 ± 0.07 μm for pH5-EWG and 0.32 ± 0.02 μm for pH9-EWG (Table 1).

On the contrary, the tortuosity parameter was significantly ($p < 0.05$) larger for the pH5-EWG (1.14 ± 0.14) than for the pH9-EWG (1.07 ± 0.01). Similarly, inter-particle aggregate distance was significantly ($p < 0.05$) longer for the pH5-EWG (1.79 ± 0.57 μm) than for the pH9-EWG (0.76 ± 0.07). This indicates smaller voids between particles in the pH9-EWG when compared to the pH5-EWG.

Thus, consistently with the qualitative analysis of the micrographs presented above, the quantitative parameters measured on the images confirm that the pH5-EWG presented both a mean particle size and an inter-particle aggregate distance significantly greater ($p < 0.05$) than

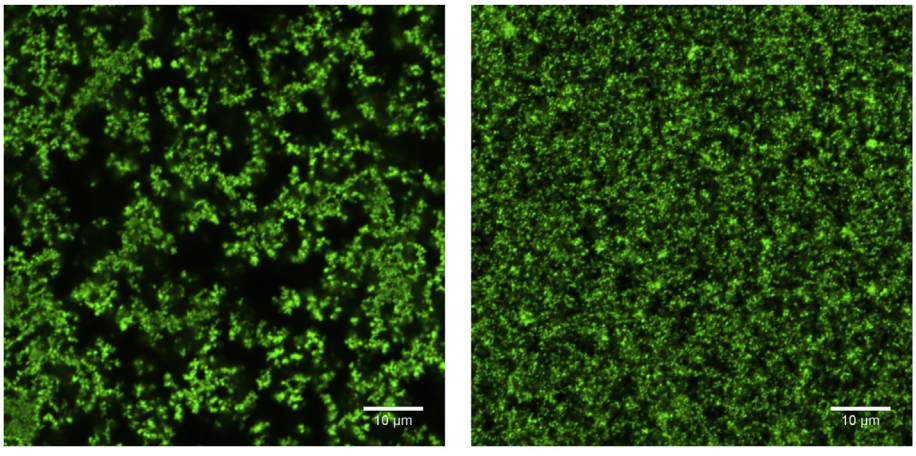

Fig. 2. PH5-EWG (a) and pH9-EWG (b) micrographs obtained from the confocal imaging.

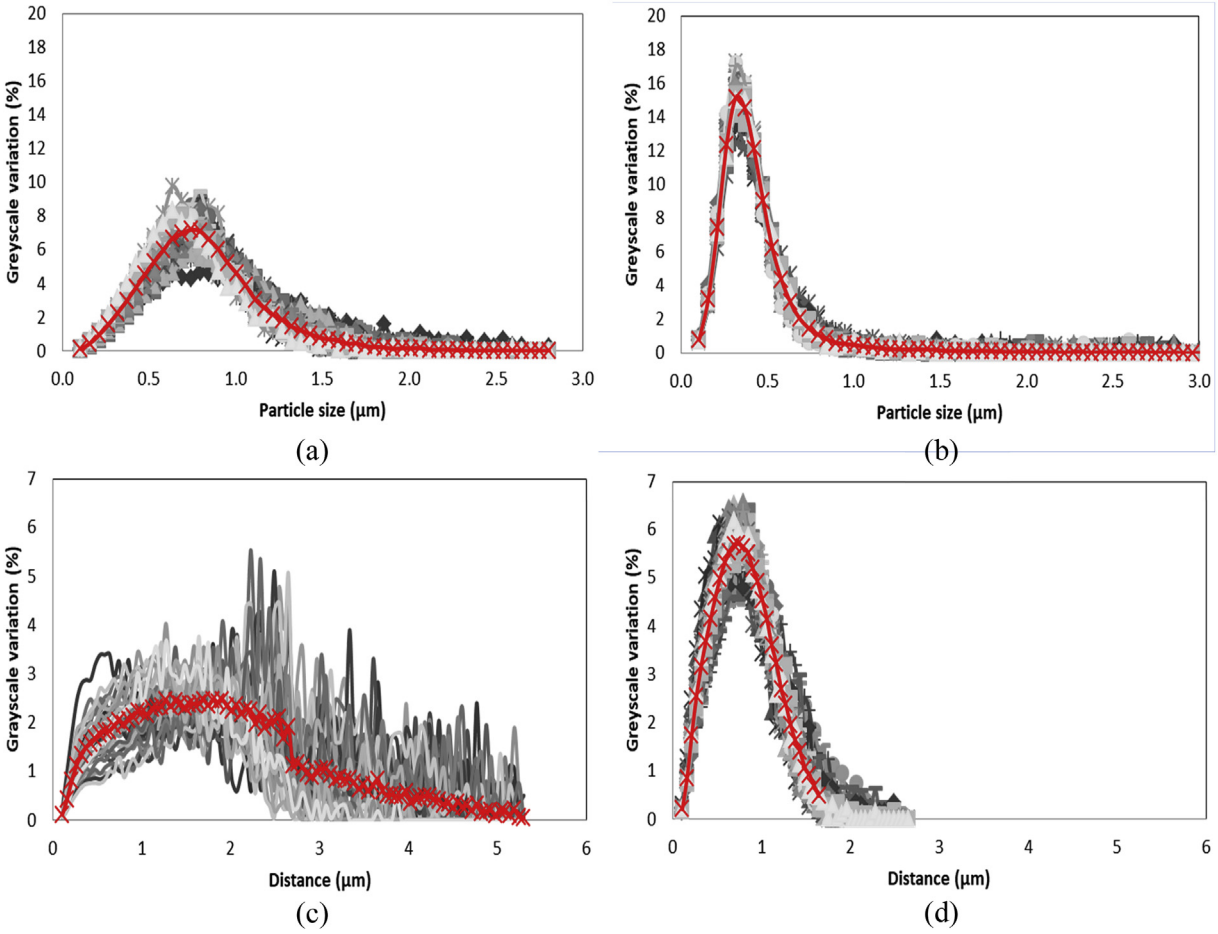

Fig. 3. Distribution of particle aggregate sizes (μm) in confocal micrographs of (a) pH5-EWG and (b) pH9-EWG. Distribution of inter-particle aggregate distances in confocal micrographs of (c) pH5-EWG and (d) pH9-EWG. The average curve (red solid line) of each graph was obtained from 30 individual curves (grey solid lines). (For interpretation of the references to colour in this figure legend, the reader is referred to the Web version of this article.)

that for the pH9-EWG. Moreover, Fig. 3 highlights broader distributions of both particle size and inter-particle aggregate distance for the pH5-EWG, meaning that this latter EWG is more heterogeneous than the pH9-EWG. The dense and homogeneous structure of the pH9-EWG, made of small protein aggregates with abundant small pores, explains the lower tortuosity value of this gel than that of the pH5-EWG, made of non-homogeneously distributed large protein aggregates and many interconnected large pores.

These results are very much in line with the mechanism of globular protein heat gelation, and especillay with the impact of pH conditions on the equilibrium between the denaturation and aggregation steps that occur during such gelation (Doi, 1993). At pH5, close to the isoelectric point of most egg white proteins, electrostatic repulsions between proteins are minimal, thus favoring aggregation which leads to spherical aggregates and finally coarse particulate EWG (Nyemb, Guérin-Dubiard, et al., 2016). In contrast, at pH9, electrostatic repulsions between proteins are much higher, favoring denaturation more than aggregation, and leading to linear aggregates which produce a more homogeneous protein network (Clark, Kavanagh, & Ross-Murphy, 2001; Nyemb, Guérin-Dubiard, et al., 2016).

3.3. Effective diffusion coefficients of FITC-pepsin and FITC–dextran in EWG

Typical fluorescence recovery curves with the FITC-labeled solutes in the EWG matrices and in water are presented in Fig. 4. Diffusion profiles along with selected FRAP images before, during, and after photo-bleaching revealed distinct profiles for each gel matrices and water (Fig. 4). Nearly complete fluorescence recovery for all the FITC-pepsin and FITC-dextran curves was observed, suggesting isotropic diffusion of fluorescent molecules within gel matrices and water.

The effective diffusion coefficients obtained from the modelling of the experimental data are summarized in Table 2. The activity of the fluorescently labelled pepsin, using haemoglobin (Hb) as the substrate according to the method described in Minekus et al. (2014), was equal to zero. The enzyme was therefore fully inactivated during the labelling reaction with FITC. This may be due to the alkaline pH (around pH8) experienced by the pepsin during the labelling process. It is reported that pepsin can inactivate as a result of a completely irreversible alkaline denaturation in a narrow pH range (between pH6 and pH7) (Kamatari, Dobson, & Konno, 2003; Lin, Loy, Sussman, & Tang, 1993). Thus, FITC-pepsin diffusion does not affect the microstructure of the EWGs, and the reported values of FITC-pepsin diffusion in this study represents the effective diffusivity value within the native gels.

In agreement with the fluorescence recovery curves (Fig. 4), the calculated effective diffusion coefficient of FITC-pepsin is higher than that of FITC-dextran, regardless the treatment. The larger diffusion coefficient of FITC-pepsin compared to that of FITC-dextran may be the result of its smaller size, due to a lower molecular mass, a globular molecular shape and a smaller hydrodynamic radius (Braga, Desterro, & Carmo-Fonseca, 2004; Thevenot et al., 2017). The FITC-pepsin has a hydrodynamic radius of 3.6 nm, and the average molecular weight is 32.4 kDa (Thevenot et al., 2017). On the other hand, FITC-dextran is a linear glucose-based polysaccharide and has a hydrodynamic radius of 4.5 nm and the average molecular weight is 40 kDa (Braga et al., 2004).

The FITC-pepsin and FITC-dextran diffusion coefficients in water

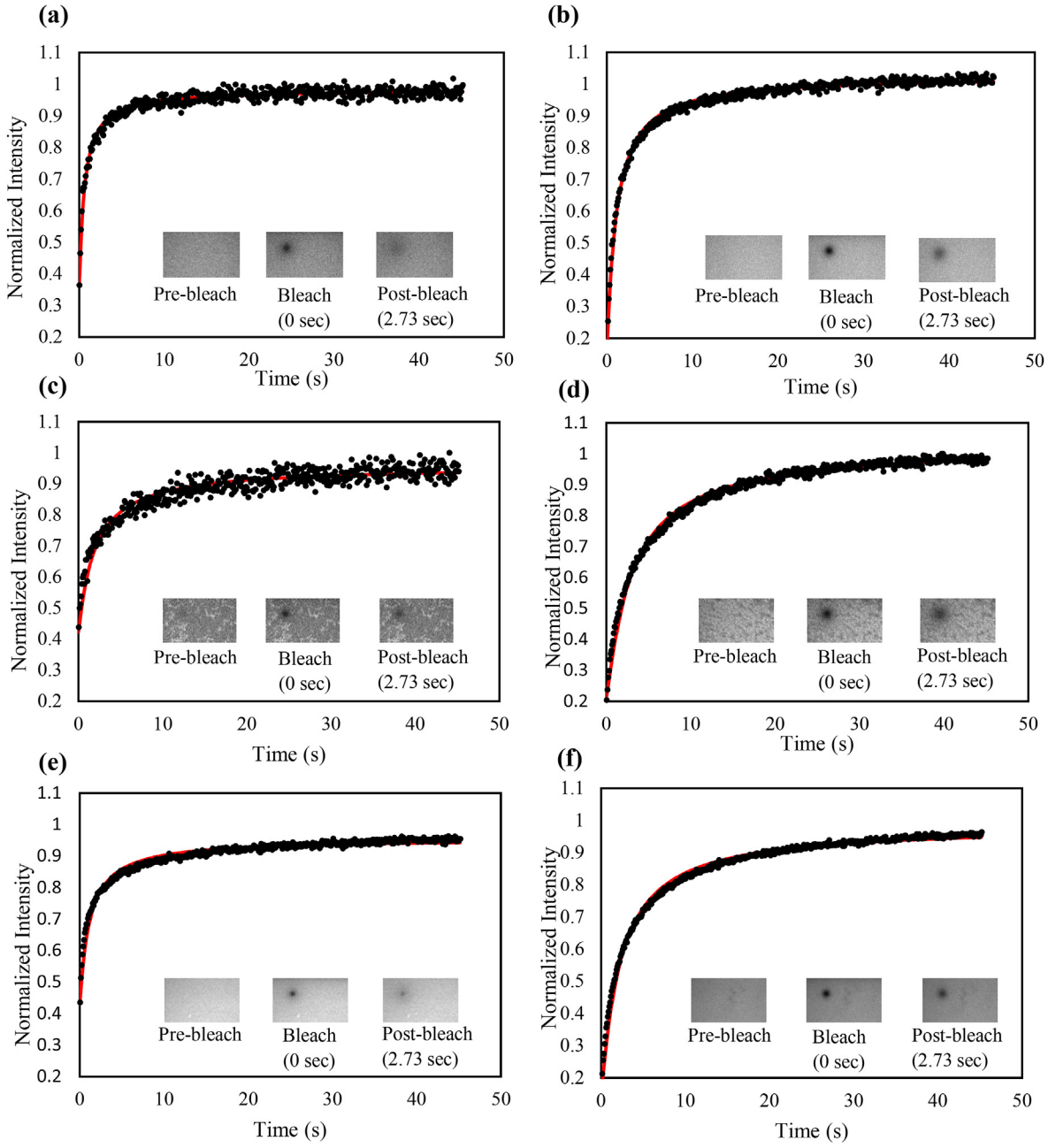

Fig. 4. Representative FRAP profiles and images before bleaching and after 0 and 2.73 s (30th post-bleaching image) for diffusion of FITC-pepsin in water (a), FITC-dextran in water (b), FITC-pepsin in pH5-EWG (c), FITC-dextran in pH5-EWG (d), FITC-pepsin in pH9-EWG (e) and FITC-dextran in pH9-EWG (f). Data points (black colour) denote the normalized experimental data and solid lines (red colour) denote the data curve fit. (For interpretation of the references to colour in this figure legend, the reader is referred to the Web version of this article.)

Table 2
Effective diffusion coefficient (D_{eff}) values relating to the mobility of FITC-pepsin and FITC-dextran in water and EWGs. Values are means ± SD (n = 30). Means within each column and raw followed by different superscript letters are significantly different ($p < 0.05$).

	Effective Diffusivity D_{eff} ($\mu m^2\ s^{-1}$)	
	FITC-pepsin	FITC-dextran
Water	104.5 ± 10.7^{a}	45.7 ± 2.1^{c}
pH5 - EWG	52.5 ± 5.3^{b}	25.9 ± 4.1^{d}
pH9 - EWG	44.2 ± 6.1^{c}	19.0 ± 3.1^{e}

are $104.5 \pm 10.7\,\mu m^2\,s^{-1}$ and $45.7 \pm 6.1\,\mu m^2\,s^{-1}$, respectively, which is in agreement with previous studies (Braga et al., 2004; Tyn & Gusek, 1990). As expected, compared with the diffusion coefficients measured in water, those measured within the EWG matrices were significantly ($p < 0.05$) lower, more particularly within the pH9-EWG. This is due to the sterical hindrance effect imposed by the microstructure of the EWGs that influences the extent of fluorescent probes mobility.

Previous studies highlighted that microstructural characteristics such as particle area fraction, pore size, pore connectivity and tortuosity are key variables required to understand the flow and transport behaviour of digestive enzymes within the food matrix (Grundy et al., 2016; Thevenot et al., 2017). In fact, results of this study show that EWGs with the same particle area fraction, but differing in tortuosity,

inter-particle aggregate distance and particle aggregate size, do not present the same efficiency for FITC-pepsin and FITC-dextran diffusion. It could be therefore hypothesized that the larger inter-connected pores and heterogeneous nature of the pH5-EWGs contribute to higher tortuosity and inter-particle aggregate distance, and thereby increased FITC-dextran and FITC-pepsin diffusivity. In contrast, the more homogeneous and dense pH9-EWG, with smaller unconnected pores, leads to smaller tortuosity and inter-particle aggregate distance, and thereby reduced the effective diffusion coefficient of FITC-dextran and FITC-pepsin.

3.4. Reduced diffusion coefficients of FITC-pepsin and FITC–dextran in EWGs

The diffusion of fluorescent probes across protein-based food systems is a multiplex phenomenon that is based on several variables, such as microstructure of the systems, shape and size of the fluorescent molecule with respect to the pore shape and size of food architecture, as well as molecular interactions (Silva et al., 2015b; Silva, Peixoto, Lortal, & Floury, 2013). Interactions between neutral FITC–dextran and the components of the protein gels were found to be negligible (Floury et al., 2012; Silva et al., 2013). However, highly pH-dependent interactions can be observed between pepsin and substrate protein molecules (Campos & Sancho, 2003; Nyemb, Guérin-Dubiard, et al., 2016; Yasnoff & Bull, 1953). Thus, in this study, FRAP-based diffusion of FITC-dextran within EWGs was used as a proxy to assess any interaction effects of FITC-pepsin and egg white protein molecules.

Table 3 shows the reduced diffusion coefficient (i.e. the ratio of effective diffusion coefficient in the gel matrix to the diffusion coefficient in water) of FITC–dextran and FITC-pepsin in the two different EWGs. The reduced diffusion coefficient is considered as an indicator of the effects of the presence of any interactions between protein particles and FITC-pepsin (if they take place) on the diffusion behaviour of the enzyme (Floury et al., 2012).

Interestingly, the reduced diffusion coefficient (Dr = 0.42) was similar for FITC-pepsin and FITC-dextran within the pH9-EWG, indicating no interaction between egg white proteins and FITC-pepsin during the diffusion process in this EWG. By contrast, the reduced diffusion coefficient was significantly ($p < 0.05$) smaller for FITC-pepsin (Dr = 0.50 ± 0.05) than for FITC-dextran (Dr = 0.57 ± 0.09) within the pH5-EWG, suggesting interactions between FITC-pepsin and this EWG matrix. Such difference between both EWGs is consistent with the modification in the net charge of the diffusing pepsin and of the main egg white proteins as a function of the pH of the system (Table 4). Most of egg white proteins are positively charged at pH5, whereas the net charge of pepsin is negative, thereby enhancing egg white proteins-pepsin electrostatic interactions. In contrast, at pH9 both egg white proteins and pepsin net charges are negative. Thus, the interactions between the FITC-pepsin and the egg protein matrix could be negligible in the pH9-EWG, due to electrostatic repulsions.

These results showed that pepsin diffusion within the gel structures is largely controlled by the egg white protein gel microstructure and to some extent by the pH conditions that determine electrostatic interactions between pepsin and egg white proteins. Thus, the loose protein network of the pH5-EWG exhibited significantly higher rate of FITC-pepsin diffusion than the more dense pH9-EWG, despite likely electrostatic interactions between pepsin and the protein network at pH5, as suggested by the lower reduced diffusion coefficient than FITC-dextran in the pH5-EWG.

Table 3
Reduced diffusion coefficient (Dr) values relating to the mobility of FITC-pepsin and FITC-dextran. Values are means ± SD (n = 30). Means within each column and raw followed by different superscript letters are significantly different ($p < 0.05$).

	Reduced diffusion coefficient (Dr)	
	FITC-pepsin	FITC-dextran
pH5 - EWG	0.50 ± 0.05^{a}	0.57 ± 0.09^{b}
pH9 - EWG	0.42 ± 0.06^{c}	0.42 ± 0.07^{c}

Table 4
Net charge of the pepsin and major egg white proteins at pH5 and pH9. The given net charge values and the estimated pI of the proteins were calculated by using the online Protein Calculator v3.4 (http://protcalc.sourceforge.net/).

	% of egg white proteins	net charge at pH 5 (mV)	net charge at pH 9 (mV)	Estimated pI
Pepsin	–	−18.0	−38.8	4.23
Lysozyme	3.5	10.8	0.2	9.04
Ovotransferrin	12.5	27.9	−33.0	7.00
Ovalbumin	54	4.2	−20.2	5.29
Ovomucoid	11	−0.3	−26.3	4.97

4. Conclusions

This study is the first reported quantitative characterization of the microstructural differences observed on EWGs of same composition but exposed to different pHs during the heat gelation process. In conclusion, results of this study indicate that, when egg white gelled at pH5, a more open and heterogeneous microstructure is formed, in comparison to the dense and more homogeneous structure of the pH9 EWG. Results further supported that pepsin diffusion in protein-based hydrogels can largely be modulated by the microstructure of the matrix, and to a less extent by the pH conditions that determine electrostatic interactions between pepsin and egg white proteins. Such knowledge could assist the food industry in developing novel protein-based formulations to control the digestion kinetics for desired health outcome. However, in the present work, we have studied the diffusion behaviour of inactivated pepsin, due to the labelling with the fluorescent dye. During gastric digestion, the pepsin is active and therefore its diffusion through the gel matrix might be accompanied by the disintegration of the EWG microstructure, and thereby might strongly influence the further pepsin mobility. There is not much information about the effect of pepsin activity on further pepsin diffusion within the food protein-based gel microstructures. As well as, research on the link between microscopic investigations of the disintegration of EWGs microstructure due to diffusion of pepsin also remains scarce and merits future investigation.

Conflict of interest and authorship conformation form

Please check the following as appropriate:

- ✓ All authors have participated in (a) conception and design, or analysis and interpretation of the data; (b) drafting the article or revising it critically for important intellectual content; and (c) approval of the final version.
- ✓ This manuscript has not been submitted to, nor is under review at, another journal or other publishing venue.
- ✓ The authors have no affiliation with any organization with a direct or indirect financial interest in the subject matter discussed in the manuscript
- ✓ The following authors have affiliations with organizations with direct or indirect financial interest in the subject matter discussed in the manuscript:

Acknowledgment

The ZEISS LSM880 confocal microscope equipped with the Fast Airyscan detector was funded by the European Union (FEDER), the

French Ministry of Education, Research and Innovation, the Regional Council of Brittany and INRA. This research work was funded by the STLO, INRA, AGROCAMPUS OUEST, Rennes, France. Geeshani Somaratne is supported by the Riddet Institute overseas placement award, New Zealand.

Appendix A. Supplementary data

Supplementary data to this article can be found online at https://doi.org/10.1016/j.foodhyd.2019.105258.

References

Abeyrathne, E., Lee, H., & Ahn, D. (2013). Egg white proteins and their potential use in food processing or as nutraceutical and pharmaceutical agents—a review. *Poultry Science, 92*(12), 3292–3299.

Akimov, M., & Bezuglov, V. (2012). Methods of protein digestive stability assay-state of the art. *New advances in the basic and clinical gastroenterology*. InTech.

Braga, J., Desterro, J. M., & Carmo-Fonseca, M. (2004). Intracellular macromolecular mobility measured by fluorescence recovery after photobleaching with confocal laser scanning microscopes. *Molecular Biology of the Cell, 15*(10), 4749–4760.

Campos, L. A., & Sancho, J. (2003). The active site of pepsin is formed in the intermediate conformation dominant at mildly acidic pH. *FEBS Letters, 538*(1–3), 89–95.

Clark, A., Kavanagh, G., & Ross-Murphy, S. (2001). Globular protein gelation—theory and experiment. *Food Hydrocolloids, 15*(4–6), 383–400.

Doi, E. (1993). Gels and gelling of globular proteins. *Trends in Food Science & Technology, 4*(1), 1–5.

Drakos, A., & Kiosseoglou, V. (2006). Stability of acidic egg white protein emulsions containing xanthan gum. *Journal of Agricultural and Food Chemistry, 54*(26), 10164–10169.

Floury, J., Madec, M. N., Waharte, F., Jeanson, S., & Lortal, S. (2012). First assessment of diffusion coefficients in model cheese by fluorescence recovery after photobleaching (FRAP). *Food Chemistry, 133*(2), 551–556.

Foegeding, E. A., & Davis, J. P. (2011). Food protein functionality: A comprehensive approach. *Food Hydrocolloids, 25*(8), 1853–1864.

Grundy, M. M., Carrière, F., Mackie, A. R., Gray, D. A., Butterworth, P. J., & Ellis, P. R. (2016). The role of plant cell wall encapsulation and porosity in regulating lipolysis during the digestion of almond seeds. *Food and Function, 7*(1), 69–78.

Guo, Q., Bellissimo, N., & Rousseau, D. (2017). Role of gel structure in controlling in vitro intestinal lipid digestion in whey protein emulsion gels. *Food Hydrocolloids, 69*, 264–272.

Guo, Q., Ye, A., Lad, M., Ferrua, M., Dalgleish, D., & Singh, H. (2015). Disintegration kinetics of food gels during gastric digestion and its role on gastric emptying: An in vitro analysis. *Food and Function, 6*(3), 756–764.

Huff, J. (2015). The airyscan detector from ZEISS: Confocal imaging with improved signal-to-noise ratio and super-resolution. *Nature Methods, 12*(12), 1205.

Inglingstad, R. A., Devold, T. G., Eriksen, E. K., Holm, H., Jacobsen, M., Liland, K. H., et al. (2010). Comparison of the digestion of caseins and whey proteins in equine, bovine, caprine and human milks by human gastrointestinal enzymes. *Dairy Science & Technology, 90*(5), 549–563.

Kamatari, Y. O., Dobson, C. M., & Konno, T. (2003). Structural dissection of alkaline-denatured pepsin. *Protein Science, 12*(4), 717–724.

Korobchevskaya, K., Lagerholm, B. C., Colin-York, H., & Fritzsche, M. (2017). Exploring the potential of airyscan microscopy for live cell imaging. *Photonics, 4*(3), 41.

Legland, D., Arganda-Carreras, I., & Andrey, P. (2016). MorphoLibJ: Integrated library and plugins for mathematical morphology with ImageJ. *Bioinformatics, 32*(22), 3532–3534.

Legland, D., Devaux, M. F., Bouchet, B., Guillon, F., & Lahaye, M. (2012). Cartography of cell morphology in tomato pericarp at the fruit scale. *Journal of Microscopy, 247*(1), 78–93.

Lin, X., Loy, J. A., Sussman, F., & Tang, J. (1993). Conformational instability of the N- and C-terminal lobes of porcine pepsin in neutral and alkaline solutions. *Protein Science, 2*(9), 1383–1390.

Lorieau, L., Halabi, A., Ligneul, A., Hazart, E., Dupont, D., & Floury, J. (2018). Impact of the dairy product structure and protein nature on the proteolysis and amino acid bioaccessiblity during in vitro digestion. *Food Hydrocolloids, 82*, 399–411.

Luo, Q., Borst, J. W., Westphal, A. H., Boom, R. M., & Janssen, A. E. (2017). Pepsin diffusivity in whey protein gels and its effect on gastric digestion. *Food Hydrocolloids, 66*, 318–325.

Matsuoka, R., Takahashi, Y., Kimura, M., Masuda, Y., & Kunou, M. (2017). Heating has no effect on the net protein utilisation from egg whites in rats. *Science World Journal,* 6817196. https://doi.org/10.1155/2017/6817196.

Minekus, M., Alminger, M., Alvito, P., Ballance, S., Bohn, T., Bourlieu, C., et al. (2014). A standardised static in vitro digestion method suitable for food–an international consensus. *Food and Function, 5*(6), 1113–1124.

Nyemb, K., Causeur, D., Jardin, J., Briard-Bion, V., Guérin-Dubiard, C., Rutherfurd, S. M., et al. (2016a). Investigating the impact of egg white gel structure on peptide kinetics profile during in vitro digestion. *Food Research International, 88*, 302–309.

Nyemb, K., Guérin-Dubiard, C., Pézennec, S., Jardin, J., Briard-Bion, V., Cauty, C., et al. (2016b). The structural properties of egg white gels impact the extent of in vitro protein digestion and the nature of peptides generated. *Food Hydrocolloids, 54*, 315–327.

Nyemb, K., Rutherfurd, M. S., Guérin, C., Dupont, D., & Nau, F. (2015). How the matrix characteristics of egg white gel influence the in vivo gastric digestion process: Spatio-temporal mapping. *6. International symposium on "delivery of functionality in complex food systems: Physically inspired approaches from the nanoscale to the microscale"*.

Opazo-Navarrete, M., Altenburg, M. D., Boom, R. M., & Janssen, A. E. (2018). The effect of gel microstructure on simulated gastric digestion of protein gels. *Food Biophysics, 13*(2), 124–138.

Silva, J. V., Legland, D., Cauty, C., Kolotuev, I., & Floury, J. (2015a). Characterization of the microstructure of dairy systems using automated image analysis. *Food Hydrocolloids, 44*, 360–371.

Silva, J. V., Lortal, S., & Floury, J. (2015b). Diffusion behavior of dextrans in dairy systems of different microstructures. *Food Research International, 71*, 1–8.

Silva, J. V. C., Peixoto, P., Lortal, S., & Floury, J. (2013). Transport phenomena in a model cheese: The influence of the charge and shape of solutes on diffusion. *Journal of Dairy Science, 96*(10), 6186–6198.

Thevenot, J., Cauty, C., Legland, D., Dupont, D., & Floury, J. (2017). Pepsin diffusion in dairy gels depends on casein concentration and microstructure. *Food Chemistry, 223*, 54–61.

Tomczyńska-Mleko, M., Handa, A., Wesołowska-Trojanowska, M., Terpiłowski, K., Kwiatkowski, C., & Mleko, S. (2016). New controlled release material: Aerated egg white gels induced by calcium ions. *European Food Research and Technology, 242*(8), 1235–1243.

Tyn, M. T., & Gusek, T. W. (1990). Prediction of diffusion coefficients of proteins. *Biotechnology and Bioengineering, 35*(4), 327–338.

Yasnoff, D. S., & Bull, H. B. (1953). Interaction of egg albumin and pepsin. *Journal of Biological Chemistry, 200*(2), 619–628.